Astron. Astrophys. 302, 58–68 (1995)

ASTRONOMY AND ASTROPHYSICS

Circum-nuclear gas flows in NGC 4151*

B. Vila-Vilaró[1], A. Robinson[2], E. Pérez[3,4], D.J. Axon[5,6], S.A. Baum[7], R.M. González-Delgado[3,4], A. Pedlar[5], I. Pérez-Fournon[3], J.J. Perry[2], and C.N. Tadhunter[8]

[1] Nobeyama Radio Observatory, Nagano 384-13, Japan
[2] Institute of Astronomy, Madingley Road, Cambridge CB30HA, UK
[3] Instituto de Astrofísica de Canarias, 38200 La Laguna, Tenerife, Spain
[4] Instituto de Astrofísica de Andalucia, Aptdo. 3004, 18080 Granada, Spain
[5] Nuffield Radio Astronomy Laboratory, Jodrell Bank, Macclesfield, Cheshire SK119DL, UK
[6] Affiliated to the Astrophysics Division of ESA, Space Telescope Science Institute, 3700 San Martin Drive, Baltimore, MD 21218, USA
[7] Space Telescope Science Institute, 3700 San Martin Drive, Baltimore, MD 21218, USA
[8] Department of Physics, University of Sheffield, Sheffield S37RH, UK

Received 19 September 1994 / Accepted 31 January 1995

Abstract. We report broad-band imaging observations which reveal a circum-nuclear gas ring in NGC 4151. The ring is delineated by two arc-like features probably resulting from dust extinction of the background stellar continuum. These features are distributed along opposite quadrants of an elliptical ring which has a semi-major axis of length 1.8 kpc and is approximately aligned with the NE-SW axis of elongation of the extended emission line region. We discuss this ring in relation to the spatial distribution and kinematics of both ionized and neutral gas components as revealed by published optical spectroscopy and 21 cm observations. These data allow us to form a coherent picture of the gas flows in the circum-nuclear environment of NGC 4151 which is strikingly similar to numerical simulations of streaming induced by barred potentials in which the $x2$ family of orbits is well developed. On this basis, we propose that the distribution of gaseous material in the galactic bar of NGC 4151 traces the path by which the gas is transported towards the active nucleus. The alignment between the circum-nuclear ring and the ENLR can then be seen as a strong indication that the collimation of the ionizing radiation field of the active nucleus is related to the dynamical parameters of the galactic bar. Specifically, we propose that bar-driven gas flows create the opaque torus which is believed to collimate the radiation field.

Key words: galaxies: active – galaxies: Seyfert – galaxies: individual (NGC 4151) – galaxies: ISM – galaxies: kinematics and dynamics

Send offprint requests to: A. Robinson, Division of Physical Sciences, University of Hertfordshire, College Lane, Hatfield, Hertfordshire AL 10 9 AB, UK. e-mail: ar@star.herts.ac.uk

* This paper is based on work carried out by the LAG (Lovers of Active Galaxies) collaboration. LAG is a consortium of mainly European astronomers which was established to study active galaxies using the International Time allocation at the Canary Islands' observatories operated under the auspices of the Comité Científico Internacional.

1. Introduction

The interplay between active galactic nuclei and their host galaxies is clearly of fundamental importance to the processes which determine the structure and evolution of these systems. To highlight just two aspects of the relationship, the interstellar medium of the host is potentially a vast reservoir of fuel for the activity occurring in the nucleus, while on the other hand, the interstellar medium may be ionized and heated by radiation escaping in a collimated beam from the nucleus. In order to elucidate the nature of the interactions which must take place between the active nucleus and its circum-nuclear environment, the LAG collaboration is engaged in a detailed study of the nearby Seyfert 1 galaxy NGC 4151. In previous papers (Penston et al. 1990; Robinson et al. 1994), we have concentrated on the extra-nuclear emission line region (ENLR), which extends approximately 2 kpc either side of the nucleus along the NE-SW axis. By a detailed analysis of long-slit spectra we have demonstrated that this gas is indeed photoionized by the active nucleus, and we have inferred a plausible geometry explaining the illumination of the galactic disk by the ionizing radiation beam. Here we concentrate on the neutral or weakly ionized gaseous material surrounding the nucleus. In particular, we report a new result based on broad-band imaging which seems to indicate a connection between galactic scale gas transfer towards the active nucleus and the collimation of the ionizing radiation field.

Several mechanisms have been proposed to explain the fuelling of the supermassive black hole in the standard model of

nuclear activity. They can be broadly divided into those which utilize local sources of fuel, such as a dense nuclear star cluster closely surrounding the black hole itself, and those that involve the transfer of gas from the interstellar medium of the galaxy as a whole (Perry 1993; Shlosman et al. 1990). Nuclear starbursts surrounding supermassive black holes have been invoked as a solution to the problem of creating the broad emission line region (Perry & Dyson 1985); such events can also provide fuel for the continuum source via stellar mass-loss (Norman & Scoville 1988; Williams & Perry 1994). However, the starburst itself requires an initial supply of gas for star formation and so we still require a mechanism for channelling material from the galactic interstellar medium into the nucleus.

Much recent attention has focused on the possibility that gravitational torques associated with stellar bars, or triggered by tidal interactions, act to drive the galactic ISM radially inwards. There is considerable circumstantial evidence to support this idea. It has been suspected for some time that Seyfert nuclei occur preferentially in barred spirals or galaxies with interacting companions (Adams 1977; Simkin et al. 1980). In a recent statistical study of known morphological features Moles et al. (1994) find that, while the incidence of bars is no greater in active galaxies than in the general population of spirals, *all* of the former show morphological peculiarities related to a non-axisymmetric potential or a tidal interaction. Moreover, CO observations show strong central concentrations of molecular material in galaxies with these morphological peculiarities (Devereux et al. 1992; Ishizuki et al. 1990; Henkel et al. 1991).

Concentrating on the role of galactic bars in particular, several recent studies based on numerical simulations (Schwarz 1985; Combes & Gerin 1985; Athanassoula 1992; Shaw et al. 1993; Friedli & Benz 1993; Shlosman & Noguchi 1993) have demonstrated that the torques set up by the non-axisymmetric gravitational potential of the bar are highly efficient at driving gaseous material into the central kiloparsec of the galaxy. Typically, the simulations show that shocks form along the leading edge of the bar. On kiloparsec scales the inflowing gas may, under certain conditions, accumulate in circum-nuclear rings, bar-like features or "spiral arms" (Athanassoula 1992), although it is far from clear how it eventually reaches the parsec scales from whence it may be accreted by the black hole. Observationally, the leading-edge shocks are seen as dust lanes (Lindblad & Jörsäter 1988; Pence & Blackman 1984-as originally suggested by Prendergast 1962), while circum-nuclear rings and bars can be traced by H II regions (or, more spectacularly, as circum-nuclear starbursts, e.g., Forbes et al. 1994) in some galaxies or inferred from CO emission (Gerin et al. 1988; Devereux et al. 1992; Kenney et al. 1992) or isophote twists (Beckman et al. 1991; Shaw et al. 1993), in others.

The subject of this paper, NGC 4151, is an early type, weakly barred spiral, SABab (de Vaucouleurs et al. 1991). The stellar bar straddles the galactic bulge in PA 130° and extends approximately 1 arc minute either side of the active nucleus (Arp 1977; Pedlar et al. 1992). On the blue plates published by Seyfert (1943) and Morgan (1968) a pair of "inner spiral arms" or "spiral segments" (cf. Schulz 1985) oriented roughly perpendicular to the main bar, can be seen close to the star-like nucleus. Similar features have been reported by Pérez-Fournon & Wilson (1990), who suggested that they may indicate a dust lane, or ring, around the ENLR.

Table 1. Properties of the broad-band filters used in the imaging of NGC 4151 and total exposure times per filter

Filter	λ_0 (Å)	$\delta\lambda_0$ (Å)	Peak trans. (%)	Total exp. (s)
U	3600	620	60	300
B	4350	1060	52	600
V	5350	940	70	720
I	8400	2000	94	540
Z	9300	1500	80	300

The multi-colour broad band imaging observations presented here clearly reveal arc-like structures located approximately 15″ to the NW and SE, respectively, of the active nucleus. They are seen most clearly as a red colour excess and largely circumscribe both the nucleus and the ENLR. We argue that these features result from extinction of the background stellar continuum by dust and propose that they delineate a circum-nuclear gas ring. We consider this structure in relation to the galactic rotation curve and the observed spatial distributions of the other gaseous components of the circum-nuclear environment. The disposition of these features is highly reminiscent of the predicted gas flows in barred potentials. We argue that the circum-nuclear ring, together with the extended narrow line region and the neutral hydrogen distribution, traces the route by which gas is transported in towards the nucleus. In particular, we discuss the implications of the close alignment between the circum-nuclear ring and the extended ionized gas for the collimation of the AGN radiation field.

2. Observations and data reduction

During the night of 5-6 May 1989 we obtained broad-band images of NGC 4151 using the Kitt Peak U, B, V, I and Gunn Z filters and a GEC CCD detector mounted at the Cassegrain focus of the 1 m Jacobus Kapteyn Telescope on La Palma. Each frame consists of 385 × 578 pixels of projected size 0.3 arcsec. Due to an autoguider failure we were forced to restrict the exposure times to a maximum of 5 minutes per frame. Several short exposures were therefore taken in each filter in order to achieve the total exposure times listed in Table 1. The individual frames were bias subtracted and flat-fielded using sky-flats. Next, each frame was then aligned with respect to that which had the narrowest point spread function and convolved with a 2-D Gaussian to match a final PSF of FWHM 1.8 arcsec. All the frames taken with the same filter were then co-added. Finally, flux calibration was performed using exposures of photometric standard stars.

A series of colour difference maps was constructed using all possible pairings of the final images. The presence of a circum-nuclear structure redder than the background continuum of the

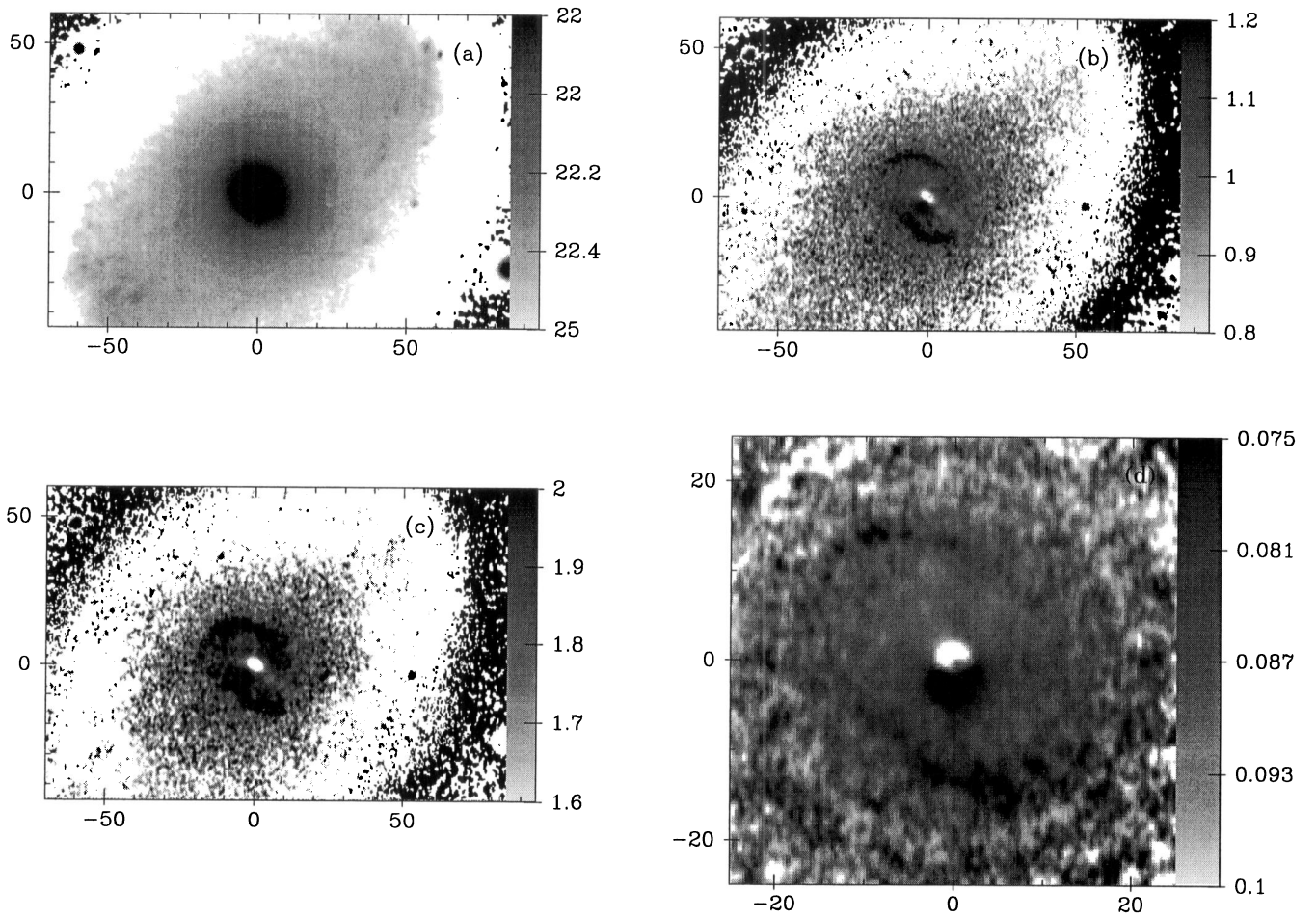

Fig. 1a–d. **a** V-band image of the nuclear region of NGC 4151. **b** $B - I$ colour map; **c** $V - I$ colour map; **d** line-free colour map obtained by dividing our I-band image by a line-free continuum image obtained by Pérez et al. (1989) in a filter centred at 5900 Å. North is up and east to the left

galactic bulge is clearly revealed in each of these difference maps. Careful examination shows that this structure corresponds to localized darkening in the V and, in particular, the B images.

The colour maps which include U, B or V-band images are contaminated by line emission. The B and V filters, in particular, include several strong emission lines (Hβ, Hγ and [Ne III]λ3869 in B; H$\beta$and [O III]$\lambda\lambda$4959, 5007 in V) from the nucleus and the extended narrow line region (ENLR) and therefore also show features resembling published narrow-band images (e.g., Pérez et al. 1989; Pérez-Fournon & Wilson 1990). However, the only significant line which falls within the I-band filter is the weaker of the [S III] doublet at 9069 Å. The equivalent width of this line in spectra of the nucleus obtained by Osterbrock, Shaw & Veilleux (1990) is only $\sim$ 5 Å. Even if its equivalent width is considerably higher off-nucleus, it is unlikely that this line contributes more than 1% of the I-band flux. Hence, in order to produce a colour map which is essentially free of emission line contamination, we have divided the I-band image by a continuum image obtained by Pérez et al. (1989) in a line-free filter centred at 5900 Å, of FWHM=490 Å.

3. Results and analysis

The V-band image of the nucleus and the colour maps $B - I$, $V - I$ and I/5900 Å are presented in Fig. 1a-d. The V image shows the active nucleus and the surrounding galactic bulge superimposed against the bar running SE-NW. In contrast, all three colour maps clearly reveal features offset to the N and S of the nucleus which are redder than the stellar continuum of the surrounding galactic bulge. The most prominent features of the colour maps are two opposed arc-like structures located at approximately equal distances to the NE and SW of the nucleus and oriented roughly perpendicular to the bar. They are clearly seen to be significant in a $B - I$ colour profile obtained from a 0.3″ slice through nucleus along the N-S axis (Fig. 2). These structures are evidently closely associated with the extremities of the ENLR. Narrow-band imaging (Pérez et al. 1989; Pérez-Fournon & Wilson 1990) shows a string of high-excitation emission line knots extending $\approx$ 20″ SW of the nucleus and more diffuse emission along a similar axis to the NE. The two red arc-like structures each begin at one pole of the NE-SW axis, where they are co-spatial with the outer edge of the ionized gas distribution, and curve in a clockwise direction towards the op-

posite pole, i.e., towards the NE from the SW pole and towards the SW from the NE pole, respectively. The "arcs" therefore appear to enclose both the nucleus and most of the ENLR. In fact, the $B-I$ map strongly suggests that these features are actually the most conspicuous segments of a broken elliptical ring. Contamination by emission lines may explain why the ring appears incomplete; both the $B-I$ and $V-I$ maps are affected by line emission inside the ring, and the breaks occur in the NE and SW where the ring intersects the ENLR.

There are two possible explanations for the red features revealed by the colour maps: they could result from the presence of a population of red supergiants, or from dust extinction of the normal stellar continuum of the galactic bulge. In the first case, the apparent red excess would indicate sites of past star formation activity. However, this seems unlikely since examination of the individual images used to construct the colour maps shows that the apparent reddening actually results from a local reduction in the blue continuum rather than an enhancement in the red. We therefore consider that dust extinction is the most likely explanation for the reddening. This is supported by a comparison of the strength of the apparent red excesses in the various colour difference maps. We have measured the colour of the red arc-like structures at several locations where no [O III] emission is seen in the narrow band image of Pérez et al. (1989). The differences in colour measured at these locations and at others with normal bulge colours at the same radial distance were then used to estimate the visual extinction, A_V. Using the standard extinction law for the Galaxy (Seaton 1979) and a value of $R = A_V/E_{B-V} = 3.2$, we have

$$\left(\frac{I_{\lambda_1}}{I_{\lambda_2}}\right)_r = \left(\frac{I_{\lambda_1}}{I_{\lambda_2}}\right)_b 10^{(\eta_{\lambda_2}-\eta_{\lambda_1})E_{B-V}/2.5}$$

where $\eta_\lambda = A_\lambda/E_{B-V}$, λ_1, λ_2 are the central wavelengths of the filters in the colour map $I_{\lambda_1}, I_{\lambda_2}$ and the subscripts r, b refer to the reddened features and the normal bulge continuum, respectively. The visual extinction was derived in this way for each colour difference map, including that formed from the I-band image and the line-free continuum at 5900 Å. The respective values of A_V are in good agreement for all combinations of colours, with a range in A_V of 0.10–0.35 magnitudes. We conclude, therefore, that the red enhancements closely follow the standard extinction law and are consistent with reddening of the bulge continuum by dust, causing a visual extinction of a few tenths of a magnitude.

Independent evidence that the red colour excess is indeed associated with dust comes from recent imaging polarimetry by Draper et al. (1992). Their data show that the distribution of polarized light in the I filter has a close spatial correspondence with the red features we have detected in the colour maps (Fig. 3). According to Draper et al., the polarization in this band is produced by dichroic absorption of background starlight by magnetically-aligned dust grains. An alternative possibility, which they consider implausible but which would still require the presence of dust, is that the polarized light is continuum radiation from the AGN which has been scattered into our line of sight.

There is evidence that faint line emission is also associated with the reddened arc-like structures. The fact that these features

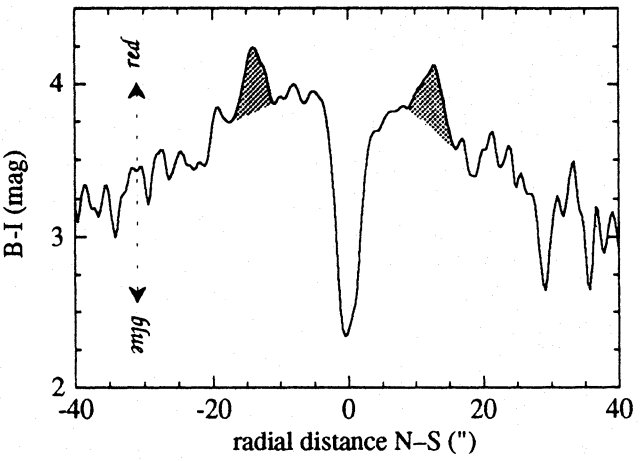

Fig. 2. $B-I$ profile taken from a radial slice of width 0.3″ through the nucleus along the N-S axis. The red excess appears as two peaks (shaded) either side of the dip corresponding to the blue nucleus

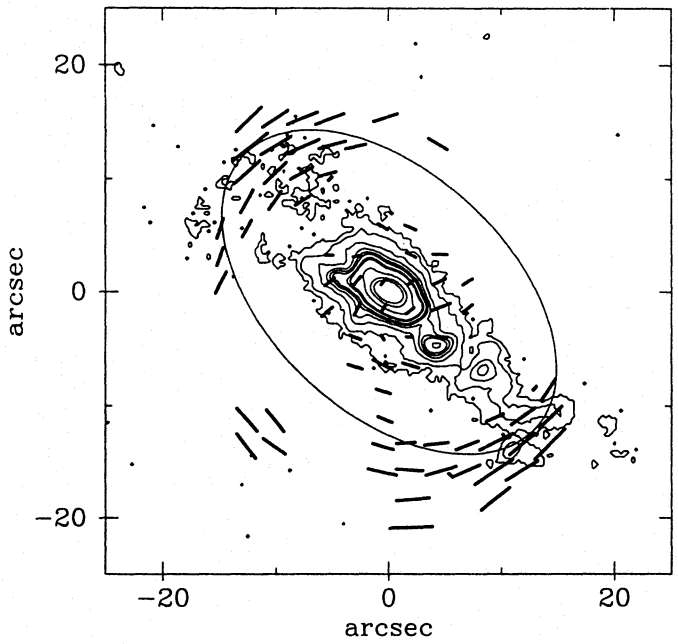

Fig. 3. Contour map of [O III]λ5007 and I-band polarization vectors from Draper et al. (1992). The red arc-like features visible in the colour maps are disposed along the NW and SE quadrants of the elliptical ring (see Fig. 1)

are clearly visible in the line-free I/5900 Å map implies that they cannot be explained solely by line emission. Nevertheless, the Hα surface brightness profile measured from a long-slit spectrum obtained by Robinson et al. (1994), centred on the bright emission line knot 6″ SW of the nucleus in PA = 135°, shows a distinct bump where the slit intercepts the south-eastern arc.

Taken together, the evidence for reddening and the detected polarization strongly suggest that the red structures trace the distribution of dust and hence of neutral or weakly ionized gas around the nucleus. In this case, a plausible interpretation of the

"inner spiral arms" which can be discerned in blue photographs (Seyfert 1943; Morgan 1968) is that they are not distinct emission features, but are delineated by extinction of stellar light from the galactic bulge by the dust arcs.

The arc-like structures give the strong impression that they form part of an elliptical ring centred on the nucleus which encloses, and is aligned with, the ENLR in PA $\approx$ 50°. The semi-major and semi-minor axes of the ellipse have lengths of 18 and 11 arcsec, respectively, or approximately 1.8 and 1.1 kpc, for $H_0 = 50\,\mathrm{km\,s^{-1}\,Mpc^{-1}}$. Note that, since the galactic disk is viewed almost face-on (Pedlar et al. 1992), the ring cannot be the projection of a circle if it lies in the plane of the disk. To explain the axial ratio, a circular ring would have to be tilted by 52° to the plane of the sky. The galactic disk is itself inclined by $\approx$ 20° to the plane of the sky (Bosma et al. 1977) and Pedlar et al. infer that the side of the disk SE of the line of nodes in PA $\approx$ 22°is tilted towards us. Therefore, if it is circular, the ring would have to be tilted by $\approx$ 30° with respect to the plane of the galactic disk. We believe it more plausible that the ring is a real ellipse co-planar with the disk. In the following, we will refer to this feature as a circum-nuclear gas ring but we would emphasize that its precise composition (i.e., the exact proportions of gas, dust or evolved stars) is largely irrelevant to the interpretation outlined in Sects. 4 and 5.

The ring apparently bears a very close spatial relationship to the ENLR: its major axis not only lies in approximately the same position angle, but its length almost precisely matches the total NE-SW extent of the ENLR as it appears in the [O III] image of Pérez et al. (1989). In fact, both the south-western and north-eastern extremities of the [O III] emission overlap the corresponding dust arcs. The line emission remains relatively bright at the SW end but is very much fainter in the NE. However, the amount of visual extinction inferred from the colour excess is only a few tenths of a magnitude at most. Thus even if the ionized gas in the SW was situated behind a uniform dust screen producing $A_V \approx 0.3$ magnitudes, the [O III] flux would only be reduced by about 30%. Similarly, the Balmer decrement would be $H\alpha/H\beta \approx 3.2$ (assuming an intrinsic recombination ratio of 2.86), which is not excluded by the existing spectroscopic data for this region (Robinson et al. 1994). Therefore, the relative brightness of the SW and NE arms of the ENLR do not necessarily indicate that the ENLR is tilted with respect to the ring such that it is actually in front of the dust in the SW, rather than co-planar with it (or behind it). More accurate measurements of the Balmer decrement in the overlap regions will be required in order to settle this question.

4. The circum-nuclear environment

We next consider the circum-nuclear ring within the general context of the interstellar medium surrounding the active nucleus. We have already noted that this structure is closely associated with the ionized gas in the ENLR. We now discuss how these components relate to the neutral gas in the galactic bar. In addition, we assess the kinematic evidence for dynamical resonances and streaming motions induced by the bar, using results from both 21 cm and optical long-slit observations.

4.1. The distribution of gas and dust

The major axis of the stellar bar in NGC 4151 lies along PA $\approx$ 130°, almost perpendicular to the common axis of the ENLR and the dust ellipse. The galaxy as a whole is almost face-on, with the disk inclined by approximately 20° (Bosma et al. 1977) to the plane of the sky and the line of nodes oriented along position angle $\approx$ 22°. Very deep plates obtained by Arp (1977) reveal that the faint spiral arms begin at the ends of the bar. Both the bar and the spiral arms are clearly seen as structures in emission from the neutral hydrogen 21 cm line (Davies 1973; Bosma et al. 1977; Pedlar et al. 1992).

The data recently obtained by Pedlar et al. (1992) have sufficient spatial resolution to allow the major features of the neutral hydrogen distribution within the galactic bar to be discerned. The overall H I morphology resembles a patchy elliptical ring of dimensions $3 \times 2'$, centred on the nucleus, and with its major axis along the bar in PA $\approx$ 130°. The most intense emission occurs along two "arms", located in opposite quadrants of the H I ring, which connect their respective ends of the bar to opposite ends of a "bridge" of neutral hydrogen crossing the nucleus approximately along the bar minor axis (see Fig. 4b of Pedlar et al.). The latter axis is, as already noted, closely aligned with that of the circum-nuclear ring. The neutral hydrogen arms lead directly to the extremities of the ENLR and in fact appear to twist slightly around the centre in the same sense as the arc-like features seen in the colour maps. The central part of the H I bridge covering the continuum nucleus, the narrow line region and the inner parts of the ENLR, is seen in absorption against the powerful radio continuum source. Minima in the H I emission occur either side of the nucleus immediately to the NW and SE. The main components of the gas distribution within the galactic bar are sketched in Fig. 4.

As is commonly observed in barred spirals, complexes of H II regions are located near both ends of the bar, offset by some 40–60″ from the nucleus along the SE-NW axis (Schulz 1985; Pérez-Fournon & Wilson 1990; Yoshida & Ohtani 1993; Robinson et al. 1994). These H II complexes are clearly associated with the greatest concentrations of H I along the opposing "arms" (Pedlar et al. 1992; see also Fig. 4). The faint lobes of radio continuum emission recently discovered by Baum et al. (1993) seem to be roughly co-spatial with both the H I arms and the H II complexes. The spatial correspondence is not precise, and the brightest parts of this source are somewhat displaced from the H II regions, but the radio continuum lobes are generally similar in orientation and extent to the H I arms. Baum et al. interpret this radio continuum emission in terms of a starburst-driven wind from the nucleus. However, it also seems possible that at least some of it may be free-free radiation from ionized gas associated with the H II complexes.

Viewed as a whole, the spatial distribution of the gas and dust around the nucleus bears a striking similarity to numerical simulations of gas flows within barred potentials (e.g., Sanders

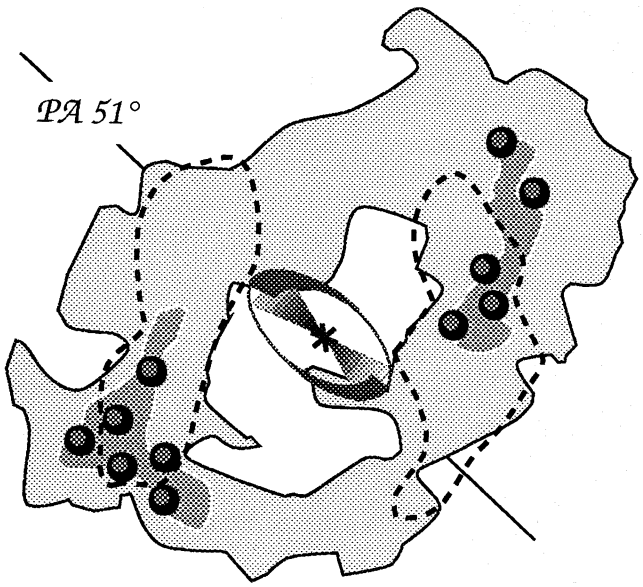

Fig. 4. Sketch showing the distribution of the main gaseous components of the galactic bar in NGC 4151. The large shaded region shows the H I distribution mapped in the 21 cm emission line by Pedlar et al. (1992). The darker shading shows the H I arms. The filled circles at the edges and along the leading sides of the bar represent the associated H II region complexes (Pérez-Fournon & Wilson 1990). The dashed lines delineate the general extent of the radio continuum lobes observed by Baum et al. (1993), omitting the unresolved core component associated with the active nucleus. The location of the active nucleus itself is indicated by a star and the protruding biconical structure in PA $\approx 50°$ represents the highly-ionized extended narrow line region (Pérez et al. 1989). The circum-nuclear gas ring revealed by our colour maps is represented by an ellipse centred on the nucleus, with the prominent arc-like structures shaded

& Tubbs 1980; Combes & Gerin 1985; Athanassoula 1992; Shaw et al. 1993). In these calculations, the gas flow is closely linked to the stable periodic orbit families and tends to be concentrated in relatively narrow streamlines along which shocks occur. The narrow dust lanes observed in barred spirals have long been identified with these shocks (Prendergast 1962). The locations of the gas streamlines are determined by the dynamical parameters of the system. A galaxy with a high central mass concentration and a weak, fat (i.e., high axial ratio), slowly rotating bar will have inner Linblad resonances (ILR). The dominant stable orbit family interior to the outermost ILR (the $x2$ family) is aligned perpendicular to the bar major axis and the longitudinal orbit family ($x1$) which supports the bar (Contopoulos & Papayannopoulos 1980). In these circumstances, offset shocks occur, with gas streamlines following the leading edges of the bar from opposite ends until, as they approach the mid-point, the opposing streams bend inwards to follow the orthogonal $x2$ orbits (e.g., Athanassoula 1992). Thus, a circum-nuclear ring of gas associated with the $x2$ orbits can form with its major axis oriented perpendicular to that of the bar.

The situation in NGC 4151 corresponds extremely well with the class of models outlined above. The presence of a bulge argues for a high central mass concentration, while the bar has relatively large axial ratio ($\sim 1:2$), although its pattern speed is difficult to determine (cf. Sect. 4.2). The locations of the H II regions, mainly near the ends of the bar, are in accord with the simulations, which suggest that star formation should occur preferentially at these sites because of the relatively low shear. More importantly, however, the spatial distribution of gaseous material in the bar closely matches the predicted gas streamlines. Pedlar et al. (1992) have already suggested that the H I arms can be identified with the leading-edge shocks and that the "bridge" across the nucleus may be associated with the $x2$ orbits. Our discovery of red arc-like features curved around an ellipse oriented approximately perpendicular to the bar major axis, and apparently contiguous with the H I arms (Fig. 4), adds considerable weight to this interpretation. In the context of Athanassoula's (1992) numerical simulations, we may identify the arcs with the inner ends of the gas streamlines, where they change direction to follow the $x2$ orbits. The simulations typically show gas distributed in a ring around the galactic centre, but the highest concentrations occur in opposite quadrants where the streamlines join the ring, exactly where the arcs appear in NGC 4151.

Although the numerical simulations indicate that the inflowing gas tends to form a ring within the outermost ILR, the interior is not devoid of gas. Indeed, the rings produced in Athanassoula's simulations can be quite thick. Similarly, calculations by Shaw et al. (1993), which also take into account the gravitational effects of the gas itself, show that for a model characterized by a high central mass concentration and, consequently, two ILRs, the gas accumulates in elongated orbits between the two resonances and forms an inner bar-like structure. If, as we will argue below, a similar situation appertains in NGC 4151, we can incorporate the ENLR into the overall picture as the consequence of photoionization of a part of such a gaseous bar by the ionizing radiation field of the Seyfert nucleus. The fact that the ionized gas is confined to a relatively narrow "jet", rather than filling the whole of the region enclosed by the circum-nuclear ring, may be explained in terms of the geometry deduced by Robinson et al. (1994) according to which the ionizing radiation escapes from the nucleus in a broad cone inclined at grazing incidence to the galactic disk. This raises the intriguing question as to why the radiation field is collimated in such a way as to produce a zone of ionized gas which is closely aligned with the major axis of the ring. However, we defer a discussion of this issue to Sect. 5.

Contrary to the predictions for a purely stellar system, the major axis of the circum-nuclear ring is not precisely perpendicular to the main galactic bar. This slight mis-alignment could be a projection effect, since the disk is not quite face-on. Alternatively, it may be related to the dissipational nature of the gaseous material forming the ring; the simulations of Shaw et al. (1993) show phase shifts between the gaseous and stellar components which they attribute to cloud-cloud collisions.

4.2. Gas kinematics and the galactic rotation curve

The morphology of the gaseous material within the bar supplies convincing evidence that at least one inner Linblad resonance is

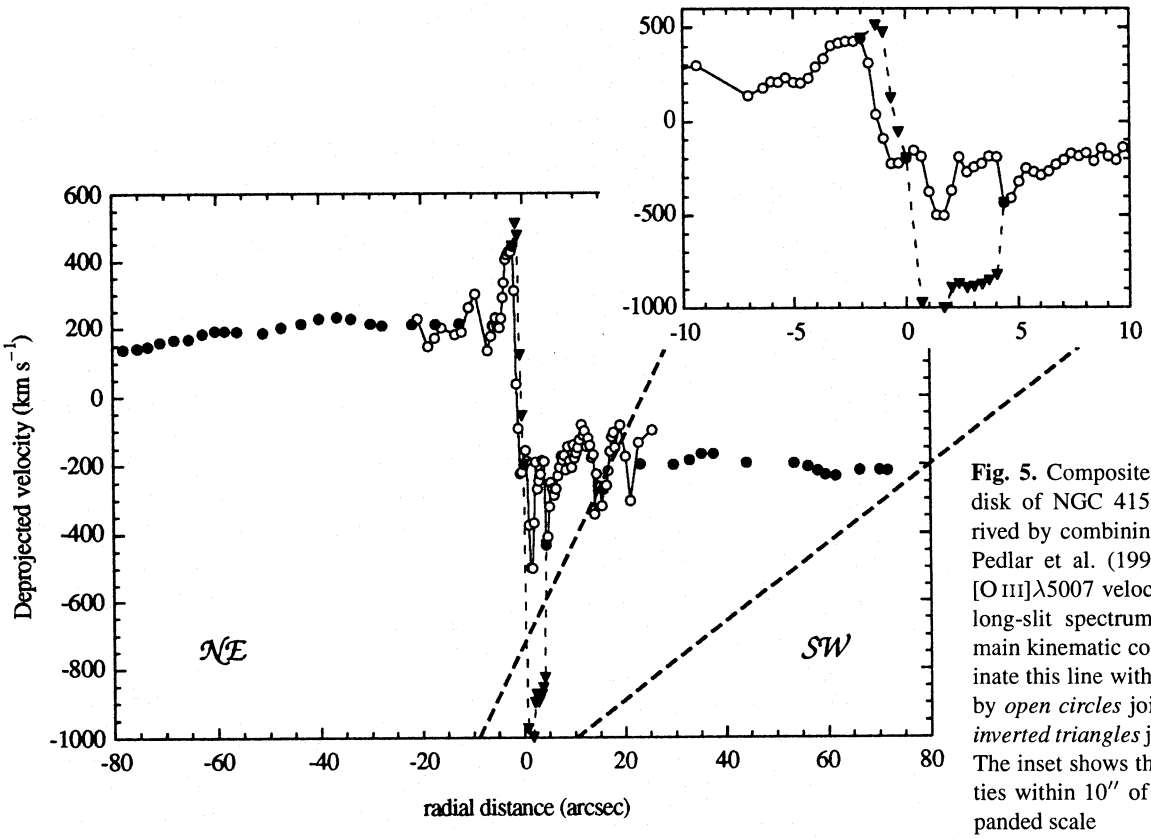

Fig. 5. Composite velocity field for the disk of NGC 4151 in PA $\approx$ 50°, derived by combining the H I velocities of Pedlar et al. (1992; *filled circles*) with [O III]λ5007 velocities measured from a long-slit spectrum (see text). The two main kinematic components which dominate this line within the NLR are shown by *open circles* joined by a full line and *inverted triangles* joined by a dashed line. The inset shows the [O III]λ5007 velocities within 10″ of the nucleus on an expanded scale

present in NGC 4151. In this case, we would expect the rotation curve to bear the signature of a high central mass concentration, since this is a necessary condition for the existence of ILRs. Indeed, if the mass concentration is such that the circular speed rises sufficiently rapidly with radius (as for a fast-rotating solid body), a second, inner, ILR may exist. As we will argue in Sect. 5, the presence of an inner ILR may have interesting consequences for the gas flows in the immediate vicinity of the nucleus. For this reason the observed rotation curve merits careful examination.

We have constructed a rotation curve for the galactic disk along the major axis of the ENLR (which is approximately the minor axis of the bar) by combining the H I velocity measurements of Pedlar et al. (1992) with a long slit spectrum obtained in PA = 51° by the LAG collaboration during a programme of spectrophotometric monitoring in 1990 (Pérez et al., in preparation; Robinson 1994). We prefer the latter data to the spectra used in our study of the ENLR (Robinson et al. 1994) because it has higher spectral ($\approx$ 1.5 Å as compared to $\approx$ 7 Å) and spatial (0.335 as compared to 1.5 arcsec pixel^{-1}) resolution, respectively, than the CCD and IPCS spectra obtained for that purpose. Furthermore, we were able to choose a spectrum from the monitoring programme which was obtained in significantly better seeing conditions ($\approx$ 0.7 arcsec) than were prevalent during the ENLR observations. The spectrum we selected was obtained at the 4.2 m William Herschel Telescope on May 2, 1990 using a 600 lines/mm grating, giving a wavelength coverage of 800 Å centred on Hβ. Details of the data reduction procedure are given in Pérez et al. (in preparation).

The composite velocity field of the neutral and ionized gas is plotted in Fig. 5. We have subtracted the systemic velocity of NGC 4151, 998 km s^{-1} (as determined by Pedlar et al., from the average H I velocities in the outer disk), corrected for heliocentric motion and deprojected the measured velocities taking the inclination and position angle of the disk to be 21° and 22°, respectively (cf. Pedlar et al. 1992).

For distances > 20″ from the nucleus, we have used H I velocities extracted from Pedlar et al.'s data cube approximately along the ENLR axis in PA $\approx$ 50°. Within a radius of 20″, we use velocities measured from the optical spectrum by fitting Gaussians to the profile of the [O III]λ5007 line. We take the position of [O III] flux peak to be the location of the nucleus. In the ENLR at distances > 5″ from the nucleus, the lines are unresolved and a single Gaussian fit suffices to determine the velocity. Allowing for the differences in spatial and spectral resolution, the velocities measured from this region agree closely with those obtained by Robinson et al. (1994). There is also excellent agreement between the optical and H I measurements, which as has already been pointed out by Pedlar et al. (1992), suggests that the ENLR kinematics are largely determined by the rotation of the galactic disk.

Within 5″ of the nucleus, contamination from the narrow line region becomes important and the ENLR emission quickly becomes subsumed into the much broader NLR profile. It is possible to trace the narrow ENLR component a little further

inwards, to about 3″ from the nucleus, by decomposing the [O III] profile into two or more Gaussians. However, within the central few arc seconds, the profile is dominated by two relatively broad components, one of which is blue-shifted by almost 1000 km s^{-1} relative to the systemic velocity (Fig. 5, inset). This feature certainly indicates large non-circular motions, and is possibly produced by an outflow (cf. Schulz 1990). The other main component of the NLR appears to link the blue-shifted ENLR SW of the nucleus with the red-shifted emission to the NE. It is conceivable that it represents a continuation of the ENLR velocity field and hence traces the galactic rotation curve within the NLR. This is by no means certain, however. Given the complex kinematics of the NLR and, in particular, the likely influence of the radio source (Pedlar et al. 1993), it is impossible to establish the rotation curve through the nucleus with much confidence.

Significant velocity perturbations are also present outside the NLR. These appear to be associated with the bright emission line knots (Robinson et al. 1994), and presumably also indicate non-circular, or non-planar, velocities. Nevertheless, the overall impression of the composite velocity field is that, beyond a distance of approximately 1/2 kpc from the nucleus, the kinematics of the ionized gas are dominated by the general rotation of the galactic disk. It is also evident that the rotation speed is roughly constant at ~ 200 km s^{-1} out to a distance of at least 8 kpc from the nucleus.

In principle, it is possible to establish the existence and locations of the Linblad resonances from the rotation curve using Lin's theory of spiral density waves (Lin et al. 1969) providing that the pattern rotation speed, Ω_p, of the bar is known. Thus, ILRs will be present if Ω_p is smaller than the maximum of the curve $\Omega(r) - \kappa/2$, where $\kappa = 2\Omega[1 + 1/2(r/\Omega)\mathrm{d}\Omega/\mathrm{d}r]^{1/2}$ is the epicyclic frequency and $\Omega(= v(r)/r)$ is the angular velocity (Binney & Tremaine 1987)[1]. Their locations are then given by the solutions to $\Omega(r) - \kappa/2 = \Omega_p$. In practice, it is difficult to extract this information from the *observed* rotation curve because both noise and real perturbations will tend to induce large deviations in $\mathrm{d}\Omega/\mathrm{d}r$. It will be evident from Fig. 5, that this is a problem for the rotation curve derived for NGC 4151. Nevertheless, it is possible to show by means of a simple but robust argument that at least one ILR must be present in this galaxy.

We proceed as follows. The most conservative statement that can be made on the basis of the data presented in Fig. 5 is that outside a radial distance of $r_c = 0.5$ kpc from the nucleus the rotation speed is everywhere approximately constant at some value v_0. The rotation curve within this radius cannot be determined because it is confused with the NLR velocity field. The angular speed is, therefore, $\Omega = v_0/r$, where $v_0 \approx 195$ km s^{-1}, the average value for the observed rotation curves beyond 0.5 kpc NE and SW of the nucleus. We next assume, in accordance with the results of several numerical simulations (Athanassoula 1992; Sellwood & Wilkinson 1993 and references therein), that the co-rotation radius is $r_{CR} \approx 1.2a$, where a is the semi-major axis of the bar. For NGC 4151 we estimate $a \approx 6.2$ kpc from the total extent of the H I ring (Pedlar et al. 1992), giving $r_{CR} \approx 7.5$ kpc and hence an angular pattern speed of $\Omega_p = v_0/r_{CR} \approx 26$ km s^{-1} kpc^{-1}. On the other hand, the angular speed at r_c is $\Omega_c \approx 390$ km s^{-1} kpc^{-1} and therefore, for a constant rotation speed, we have $(\Omega - \kappa/2)_{max} \approx \Omega_c(1 - 1/\sqrt{2}) \approx 114$ km s^{-1} kpc^{-1}. It follows that $(\Omega - \kappa/2)_{max} > \Omega_p$ and the condition for ILRs to exist is fulfilled. The location of the outermost ILR is then given by $r_{ILR} = r_{CR}(1 - 1/\sqrt{2}) \approx 2.2$ kpc. This value agrees extremely well with the morphological evidence: it is somewhat larger than the semi-major axis of the circum-nuclear gas ring ($\approx$ 1.8 kpc) but since this structure traces the $x2$ orbital family which can only exist *inside* the outermost ILR, this is precisely what we would expect.

The existence of an inner ILR is more difficult to establish with certainty, since it depends on the unknown shape of the rotation curve within the inner 0.5 kpc. It nevertheless seems probable that one is present within this radius. If we make the rather conservative assumption that the rotation speed rises linearly (i.e., as for a solid body) inside r_c to the mean value v_0, then it can be seen that $\Omega - \kappa/2 = 0$ for $r < r_c$. Consequently, $\Omega - \kappa/2$ becomes a peaked curve with a maximum $(\Omega - \kappa/2)_{max} = \Omega_c(1 - 1/\sqrt{2})$ at r_c and – since we still have $(\Omega - \kappa/2)_{max} > \Omega_p$ – inner Linblad resonances associated with both the rising and falling branches. In this case, an upper limit to the inner ILR is given by r_c. If the rotation curve increases more steeply within the inner kiloparsec than we have assumed, then the inner ILR may be considerably closer to the nucleus.

The rotation curve indicates that ILRs should exist in NGC 4151, as is necessary to induce the flow patterns inferred from the circum-nuclear distribution of gaseous material. These flow patterns imply important streaming motions which should be apparent as perturbations in the rotational velocity field. The fact that NGC 4151 is nearly face-on makes such streaming motions difficult to detect. Nevertheless, Pedlar et al. (1992) note that the H I velocity field exhibits significant departures from coplanar circular motion within the bar which could be attributed to the inferred gas flows. We have used Pedlar et al.'s data to examine the distribution of peculiar velocities in more detail. A 2-D model for the global rotation of the disk based on the average rotation curve derived by Pedlar et al. was subtracted from the H I velocity field, yielding a map of the residuals (Fig. 6). Given the inclination of the disk and the position angle of the line of nodes, the presence of blue-shifted (approaching) residuals in the NW and red-shifted (receding) in the SE within the inner part of the bar are consistent with the flow pattern inferred from the morphological features (Sect. 4.1).

However, the clearest evidence for kinematical disturbances associated with the gas flows in the bar comes from the long-slit spectra presented by Robinson et al. (1994). The width of the [O III]λ5007 line, in particular, exhibits large variations along axes passing through the inner two knots (at distances of 6″ and 10″ from the nucleus) approximately perpendicular to the major axis of the ENLR (and hence of the circum-nuclear gas ring). The lines are unresolved within the knots themselves but

[1] The epicyclic approximation is not, of course, strictly valid for real galaxies but, it is adequate for the plausibility arguments discussed here.

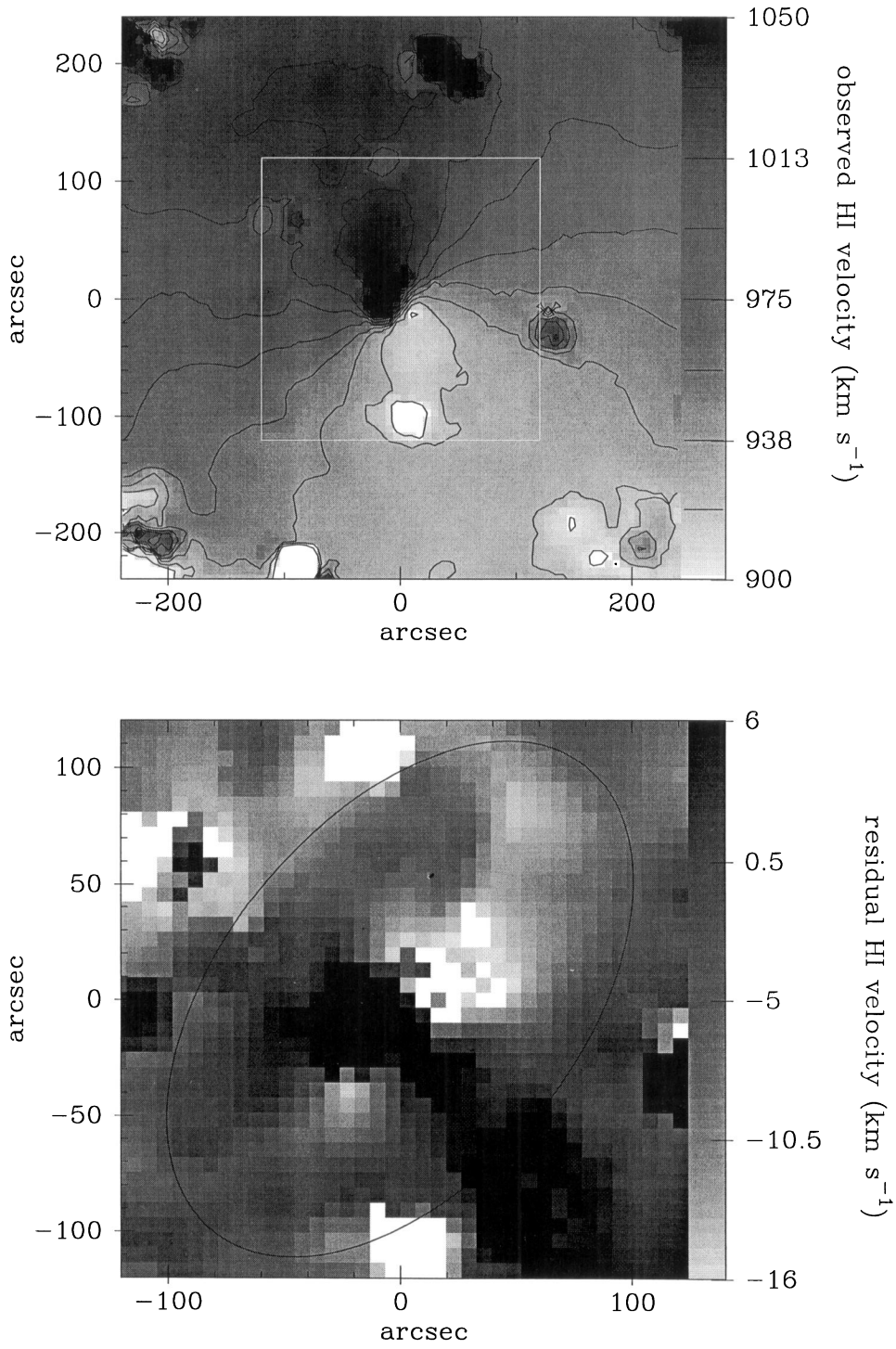

Fig. 6. Upper panel: 2-D HI velocity map of NGC 4151, obtained from the data of Pedlar et al. (1992). Lower panel: residual map of the central region (200 × 200 arcseconds; the area within the box shown in the upper panel), formed by subtracting a pure rotation model derived from the mean HI rotation curve from the observed velocity field. The approximate size and orientation of the galactic bar is indicated by the ellipse

away from the ENLR the FWHM increases by 50–100 km s^{-1}, peaking at the points where each slit intersects the ring (cf. Robinson et al., Fig. 17). The gas ring is clearly associated with a significant increase in the velocity dispersion of the emitting gas and is thus revealed as the site of enhanced dynamical activity. The numerical simulations suggest that the reddened arc-like features occur at the locations where gas streaming in from the leading edges of the bar meets that circulating in the $x2$ orbits. It therefore seems reasonable to attribute the line broadening to shocks or cloud-cloud collisions resulting from the merger of these gas flows.

5. Interpretation

The morphology of the gas and dust, together with the kinematical evidence, allow us to assemble a coherent picture of the gas

flows in the circum-nuclear environment of NGC 4151. This picture is strikingly similar to the predictions of numerical simulations of gas flows induced by barred potentials in which the $x2$ family of orbits is well developed (cf. Athanassoula 1992; Shaw et al. 1993). However, the close alignment of the ENLR with the major axis of the circum-nuclear gas ring introduces an important new element which demands an explanation. Given that the ENLR is photoionized by the AGN radiation field (e.g., Penston et al. 1990), this alignment suggests that the collimation of the ionizing radiation field and the gas flows which trace the gravitational potential of the galactic bar are intimately related.

Most existing simulations of gas flows in galactic bars lack sufficient spatial resolution to follow the flow down to scales comparable with the source of the nuclear activity (e.g., the accretion radius of the black hole $\sim 10\,pc$). Consequently, it is far from clear how the gas accumulating in a 'reservoir' at 1 kpc loses its angular momentum and eventually falls towards the centre. A number of schemes for transferring the gas into the active nucleus have been considered. Shlosman et al. (1989) have proposed that gas swept up into the inner kiloparsec by the stellar bar forms a disk which can become unstable, driving further inflow. They propose that the unstable configuration will resemble a bar-driven spiral, resulting in a gaseous "bar within a bar" and triggering gas flow along the bar towards the centre. More recently, Friedli & Martinet (1993) have used 3-D n-body simulations including both gas and stars to study in more detail the conditions under which secondary bars can form. They conclude that the presence of an ILR is essential for this to occur; the secondary bar forms when sufficient mass has accumulated in the $x2$ orbit families to decouple it from the main bar. They propose that gas can be transported deep into the nucleus by means of a hierarchy of nested bars. Alternatively, Shaw et al. (1993) have shown that in some circumstances, an inner bar can form within the ILR without decoupling from the main bar.

In NGC 4151, the presence of a circum-nuclear gas ring oriented roughly orthogonal to the galactic bar, and the evidence of the galactic rotation curve, both point to the presence of at least one, and possibly two, ILRs. The dynamical situation in this case would therefore seem to meet the conditions which, according to the models, are favourable for the formation of an inner gas bar. The ENLR could perhaps be identified with a flow along this bar. However, this cannot be the complete explanation for the alignment of the ENLR with the major axis of the gas ring, since it leaves open the question of why the gas is highly ionized only along this particular axis. It is important to realize that this is not simply a matter of the gas distribution; the observations discussed in Sect. 3 imply that neutral or weakly ionized gas is widespread around the nucleus. Rather, the ENLR morphology results from anisotropic illumination of the surrounding gas distribution by the radiation field of the active nucleus.

The geometry of the nuclear radiation field in NGC 4151 has been deduced by Vila-Vilaró (1993) and Robinson et al. (1994). According to their model, ionizing radiation escapes from the nucleus in a broad cone (of opening angle $\sim 120°$), which is inclined such that it intercepts the galactic disk at grazing incidence. The ENLR is formed within the locus of the intersection of the radiation cone with the disk. The wide opening angle is required to account for the misalignment between the ENLR (in PA $\approx 231°$) and the kiloparsec-scale nuclear radio source (in PA $\approx 257°$), assuming that the radiation beam and the radio jet have a common axis. If this model for the radiation field geometry is correct, it follows from the alignment of the ENLR with the gas ring that the axis of the radiation cone and the axis of inner gas bar are located in the same plane perpendicular to the galactic disk. This may simply be a chance alignment. But we believe it implies that the collimation mechanism of the ionizing radiation field is related to the gravitational potential of the inner few kiloparsecs of the galaxy. In particular, we postulate that the dust and gas driven in towards the nucleus by gravitational torques are the source of the opacity which is required to collimate the radiation field.

It is widely believed that radiation cones in Seyfert galaxies are produced by rings or tori of optically thick material enclosing the continuum source (e.g., Antonucci & Miller 1985; Krolik 1992). Most theoretical studies of these tori have concentrated on calculating their structure and physical conditions (e.g., Krolik & Begelman 1988; Pier & Krolik 1992). As yet, however, the question of how they are formed has received little attention. The spatial relationships between the ionized gas and the circum-nuclear ring which we have found in NGC 4151 indicate that bar-driven gas flows may play an important role in this process.

The dominant orbit family interior to the inner ILR is orthogonal to the $x2$ orbits and hence aligned with the major axis of the main bar. Since gas tends to follow the stable orbit families closely we may envisage that, just as circum-nuclear rings can form around the $x2$ orbits, gas falling in along the inner bar from the outer kiloparsec-scale ring accumulates in an *inner* circum-nuclear ring at the inner ILR. Numerical simulations by Combes & Gerin (1985) show that gas can indeed accumulate in the form of a ring at this location. The presence of an inner ILR therefore provides a straightforward mechanism which allows the incoming gas to settle into stable orbits on scales of perhaps a few tens of parsecs. We propose that this gas ring forms the opaque torus enclosing the AGN continuum source and the broad emission line region. The symmetry axis of the resulting radiation cone will coincide with the angular momentum vector of the collimating gas.

In the case of NGC 4151, the radiation cone geometry outlined above requires that this common axis must be tilted about the minor axis of the outer gas ring (i.e., the major axis of the main bar) by $\approx 30°$ relative to the rotation axis of the galactic disk, in order to create the ENLR by photoionization of gas within the disk. Given that the scale height of the gravitational potential will be much larger than the radius of the *inner* ILR, it seems quite plausible to suppose that the orbital plane of the gas within this resonance could be inclined relative to the galactic disk. The orbits might be tilted by a mechanism similar to that discussed by Tohline & Osterbrock (1982) or by vertical gravitational torques generated by the bar potential (Friedli & Benz 1993).

It is worth noting that certain results from CCD imaging of the nucleus can be interpreted as evidence for obscuration or reddening on scales of 1-2″. Pérez et al. (1989) report a belt of either low ionization or enhanced extinction crossing the nucleus in a position angle (PA $\approx$ 135°) which is close to that of the major axis of the galactic bar. In addition, Terlevich et al. (1991) find a "red bar" with a similar position angle in broad-band images. These features might conceivably be manifestations of an accumulation of dusty material around the inner ILR.

We propose, therefore, that the striking spatial relationship between the ENLR and the kiloparsec-scale circum-nuclear gas ring is not merely a coincidence but is a direct consequence of the fact that the bar-driven gas flows provide the material for the opaque torus which collimates the AGN radiation field. We may speculate that the presence and opening angle of such tori are related to the existence and strength of a second inner Linblad resonance. It seems very likely that the same gas flows trace the path by which the nuclear activity has been fuelled. Thus, the very mechanism, namely gravitational torques associated with non-axisymmetric potentials, which has been invoked to transport fuel to the continuum source may also make the resulting radiation anisotropic.

Acknowledgements. This work was made possible by a generous allocation of International Time by the *Comité Científico Internacional.* The Jacobus Kapteyn Telescope, on the island of La Palma, is operated by the Royal Greenwich Observatory at the Spanish *Observatorio del Roque de los Muchachos of the Instituto de Astrofísica de Canarias.* We are grateful to Keith Shortridge for developing and maintaining the FIGARO data reduction software, to Luis Cuesta for making the software package GRAFICOS available and to the UK SERC Starlink Project for providing computer facilities. We acknowledge financial support from the UK Science and Engineering Research Council and the *Acción Integrada* programme of the British Council and the Spanish *Ministerio de Educación y Ciencia.*

References

Adams T.F., 1977, ApJ, 33, 19
Antonucci R.R.J., Miller J.S., 1985, ApJ 297, 621
Arp A., 1977, ApJ 218, 70
Athanassoula E., 1992, MNRAS 259, 345
Baum S.A., O'Dea C.P., Dallacassa D., deBruyn A.G., Pedlar A., 1993, ApJ 419, 553
Beckman J.E., Varela A., Muñoz-Tuñón C., Vilchez J.M., Cepa J., 1991, A&A 245, 436
Binney J., Tremaine S., 1987, Galactic Dynamics, Princeton University Press
Bosma A., Ekers R.D., Lequeux J., 1977, A&A 57, 97
Combes F., Gerin M., 1985, A&A 150, 327
Contopoulos G., Papayannopoulos T., 1980, A&A 92, 33
Davies R.D., 1973, MNRAS 161, 25P
Devereux N.A., Kenney J.D. P., Young J.S., 1992, AJ 103, 784
Draper P.W., Gledhill T.M., Scarrot S.M., Tadhunter C.N., 1992, MNRAS 257, 309
Forbes D.A., Norris R.P., Williger G.M., Smith C.R., 1994, AJ 107, 984
Friedli D., Benz W., 1993, A&A 268, 65
Friedli D., Martinet L., 1993, A&A 277, 27
Gerin M., Nakai N., Combes F., 1988, A&A 203, 44
Henkel C., Baan W.A., Mauersberger R., 1991, A&AR, 3, 47
Ishizuki S., Kawabe R., Ishiguro M., et al., 1990, Nat 344, 244
Kenney J.D.P., Wilson C.D, Scoville N.Z., Devereux N., Young J.S., 1992, ApJ 395, L79
Krolik, J.H., 1992, in: Holt S.S., Neff S.G., Urry C.M. (eds.). Testing the AGN paradigm, AIP Conference Proceedings, 254, p. 473
Krolik J.H., Begelman M.C., 1988, ApJ 329, 702
Lin C.C., Yuan C., Shu F.H., 1969, ApJ 155, 721
Lindblad P.O., Jörsäter S., 1988, in: Palous J. (ed.). Evolution of Galaxies, p. 289
Moles M., Márquez I., Pérez E., 1994, ApJ 438, 604
Morgan W.W., 1968, ApJ 153, 27
Norman C., Scoville N., 1988, ApJ 332, 124
Osterbrock D.E., Shaw R.A., Veilleux S., 1990, ApJ 352, 561
Pedlar A., Howley P., Axon D.J., Unger S.W., 1992, MNRAS 259, 369
Pedlar A., Kukula M.J., Longley D.P.T., et al., 1993, MNRAS 263, 471
Pence W.D., Blackman C.P., 1984, MNRAS 207, 9
Penston M.V. et al., 1990, A&A 236, 53
Pérez E., González-Delgado R. M., Tadhunter C.N., Tsvetanov Z., 1989, MNRAS 241, 31P
Pérez-Fournon I., Wilson A.S., 1990, ApJ 356, 456
Perry J.J., 1993, in: Sandqvist Aa., Ray T.P. (eds). Central Activity in Galaxies-From Observational Data to Astrophysical Diagnostics, Springer, Berlin, p. 25
Perry J.J., Dyson J.E., 1985, MNRAS 213, 665
Pier E.A., Krolik J.H., 1992, ApJ 399, L23
Prendergast K.H., 1962, unpublished
Robinson A., 1994, in: Reverberation Mapping of the Broad-Line Region of AGN, Gondhalekar P.M., Horne K., Peterson B.M. (eds.). ASP Conf. Ser. 69, p 147
Robinson A., Vila-Vilaró B., Axon D.J., et al., 1994, A&A 291, 351
Sanders R.H., Tubbs A.D., 1980, A&A 235, 803
Schulz H., 1985, A&A 143, 29
Schulz H., 1990, AJ 99, 1442
Schwarz M.P., 1985, MNRAS 212, 677
Seaton M.J., 1979, MNRAS 187, 73P
Sellwood J.A., Wilkinson A., 1993, Rep. Prog. Phys., 56, 173
Seyfert C.K., 1943, ApJ 97, 28
Shaw M.A., Combes F., Axon D.J., Wright G.S., 1993, A&A 273, 31
Shlosman I., Begelman M.C., Frank J., 1990. Nat 345, 679
Shlosman I., Frank J., Begelman M.C., 1989, Nat 338, 45
Shlosman I., Noguchi N., 1993, ApJ 414, 474
Simkin S., Su H., Schwarz M.P., 1980, ApJ 237, 404
Terlevich R.J., Sánchez-Portal M., Díaz A.I., Terlevich, E., 1991, MNRAS 249, 36
Tohline J.E., Osterbrock D.E., 1982, ApJ 252, L49
de Vaucouleurs G., de Vaucouleurs A., Corwin H.G., et al., 1991, Third Reference Catalogue of Bright Galaxies, Springer, New York
Vila-Vilaró B., 1993, Ph.D. thesis, University of La Laguna
Williams R.J.R., Perry J.J., 1994, MNRAS 269, 538
Yoshida M., Ohtani H., 1993, PASJ, 45, 407